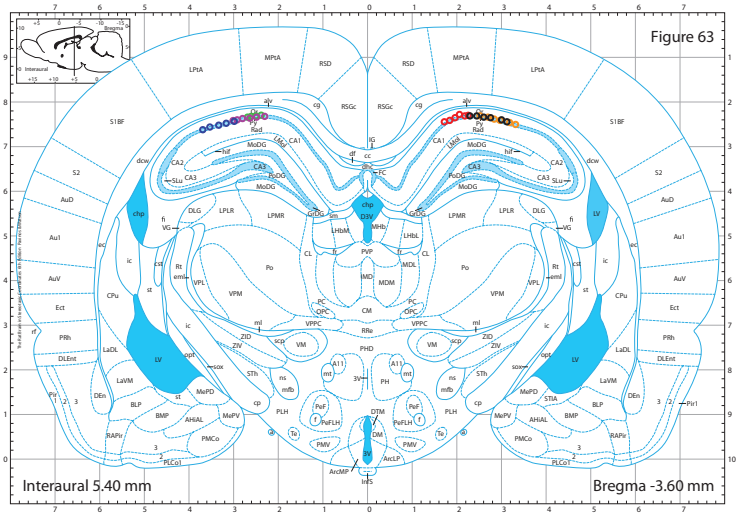
Figure 63
Interaural 5.40 mm
Bregma -3.60 mm

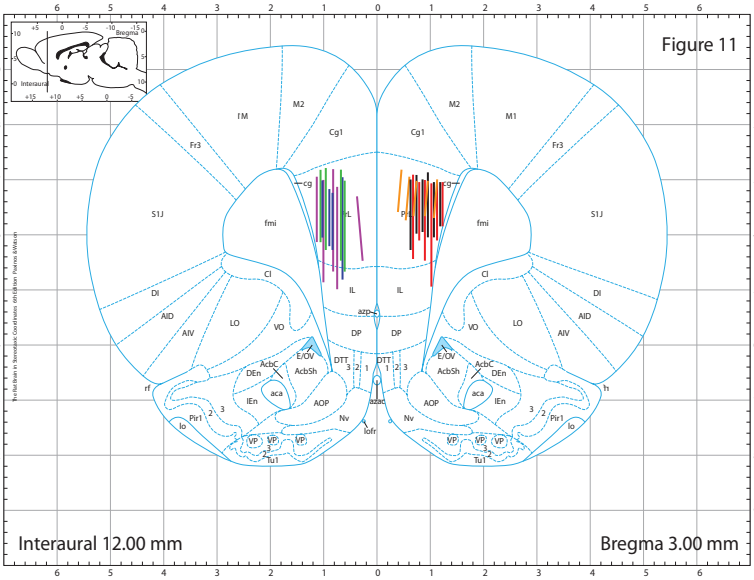
Figure 11
Interaural 12.00 mm
Bregma 3.00 mm

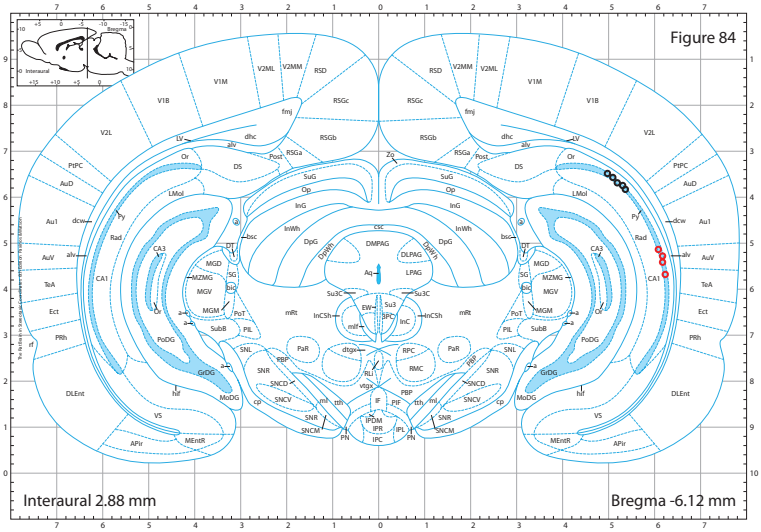
Figure 84
Interaural 2.88 mm
Bregma -6.12 mm

Figure S1

Figure S1 (related to Figure 1): Schematic of recording locations.

Recording locations projected on to coronal atlas sections for dorsal CA1 (top panel), PFC (middle panel, lines mark path of tetrode advancement across days), and intermediate CA1 (bottom panel). W-track animals: black, red and orange. Y-track animals: purple, green and blue. Note that W-track recordings are in right hemisphere, and Y-track recordings are in left hemisphere.

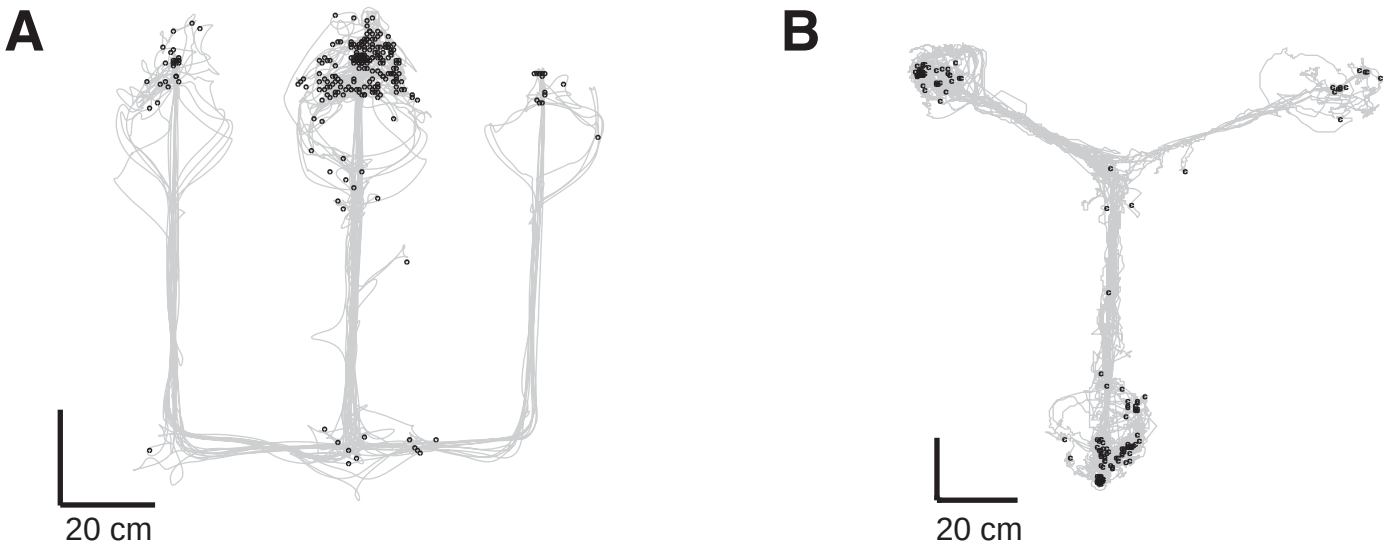

Figure S2

Figure S2 (related to Figure 2): Location of SWRs.

(A) A representative W-track session illustrating location of SWRs overlaid over all positions on the track visited by the animal.

(B) A representative Y-track session.

The fraction of SWRs that occurred at reward wells was 0.76 ± 0.02 (mean ± sem, n = 53 days), with a small but significant difference in the two tasks (0.71 ± 0.03 for the W-track task with n = 24 days, and 0.79 ± 0.02 for the Y-track task with n = 29 days; p = 0.03, rank-sum test).

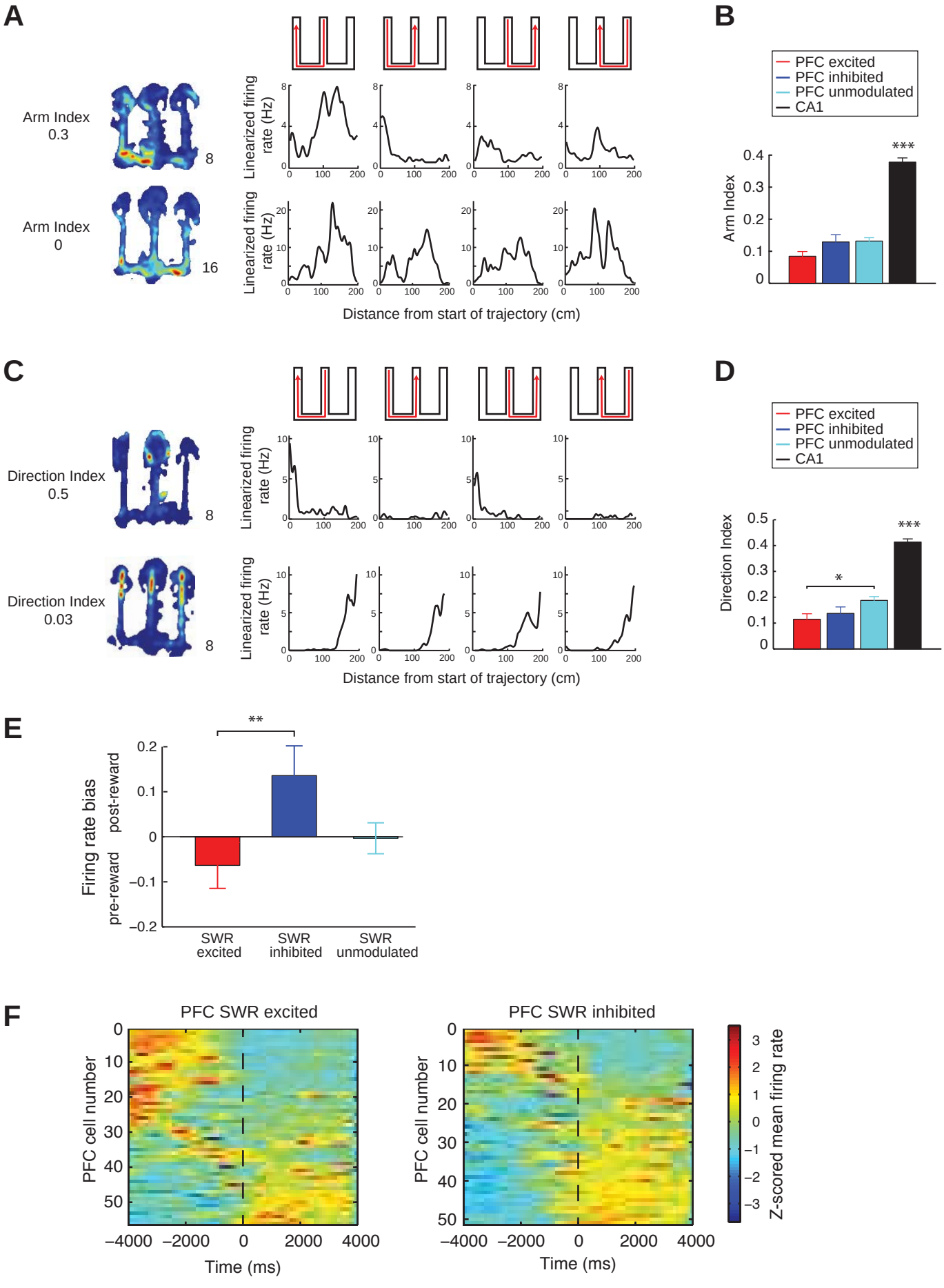
A
Arm Index
0.3
8
Arm Index
0
16
Linearized firing rate (Hz)
Distance from start of trajectory (cm)
B
PFC excited
PFC inhibited
PFC unmodulated
CA1
Arm Index
***
C
Direction Index
0.5
8
Direction Index
0.03
8
Linearized firing rate (Hz)
Distance from start of trajectory (cm)
D
PFC excited
PFC inhibited
PFC unmodulated
CA1
Direction Index
*
***
E
Firing rate bias
pre-reward
post-reward
**
SWR excited
SWR inhibited
SWR unmodulated
F
PFC SWR excited
PFC SWR inhibited
PFC cell number
Time (ms)
Z-scored mean firing rate

Figure S3

Figure S3 (related to Figure 5): Spatial and Behavioral Coding Properties of PFC Populations.

(A) 2D and linearized firing rate maps of example PFC cells with low and high arm selectivity. Each row corresponds to one cell. The linearized firing rates are shown for the 4 trajectories on the track schematized above.

(B) Mean arm selectivity in the PFC and CA1 populations. The CA1 population is also shown for comparison, and has significantly higher arm selectivity than all the PFC populations (***p< 10-4, rank-sum test).

(C) 2D and linearized firing rate maps for example PFC cells with high and low directional firing indices. Each row corresponds to a single neuron.

(D) Mean direction selectivity in the PFC and CA1 populations. The CA1 population has significantly higher direction selectivity than all the PFC populations (***p< 10-4, rank-sum test). SWR-excited neurons have significantly lower direction selectivity than SWR-unmodulated neurons (*p< 0.01, rank-sum test).

(E) Reward modulation index for SWR-excited (n = 56), SWR-inhibited (n = 51) and SWR-unmodulated (n = 194) PFC cells. Firing rate modulation index quantifies difference in post-reward periods (0 to 2 secs after reward) and pre-reward periods (-3 to -1 sec before reward). Index varies between -1 to +1, with +1 indicating firing only in the post-reward window and -1 indicating firing only during pre-reward (**p = 0.007, rank-sum test).

(F) Reward-triggered mean firing of SWR-excited and SWR-inhibited PFC cells. Each row shows the z-scored mean reward-triggered (reward at time 0) firing of one neuron. Neurons are ordered by their firing amplitude in a 0-2 sec window after reward onset. A greater fraction of SWR-inhibited neurons are reward selective as compared to SWR-excited neurons, resulting in a higher reward modulation index shown in **E**.

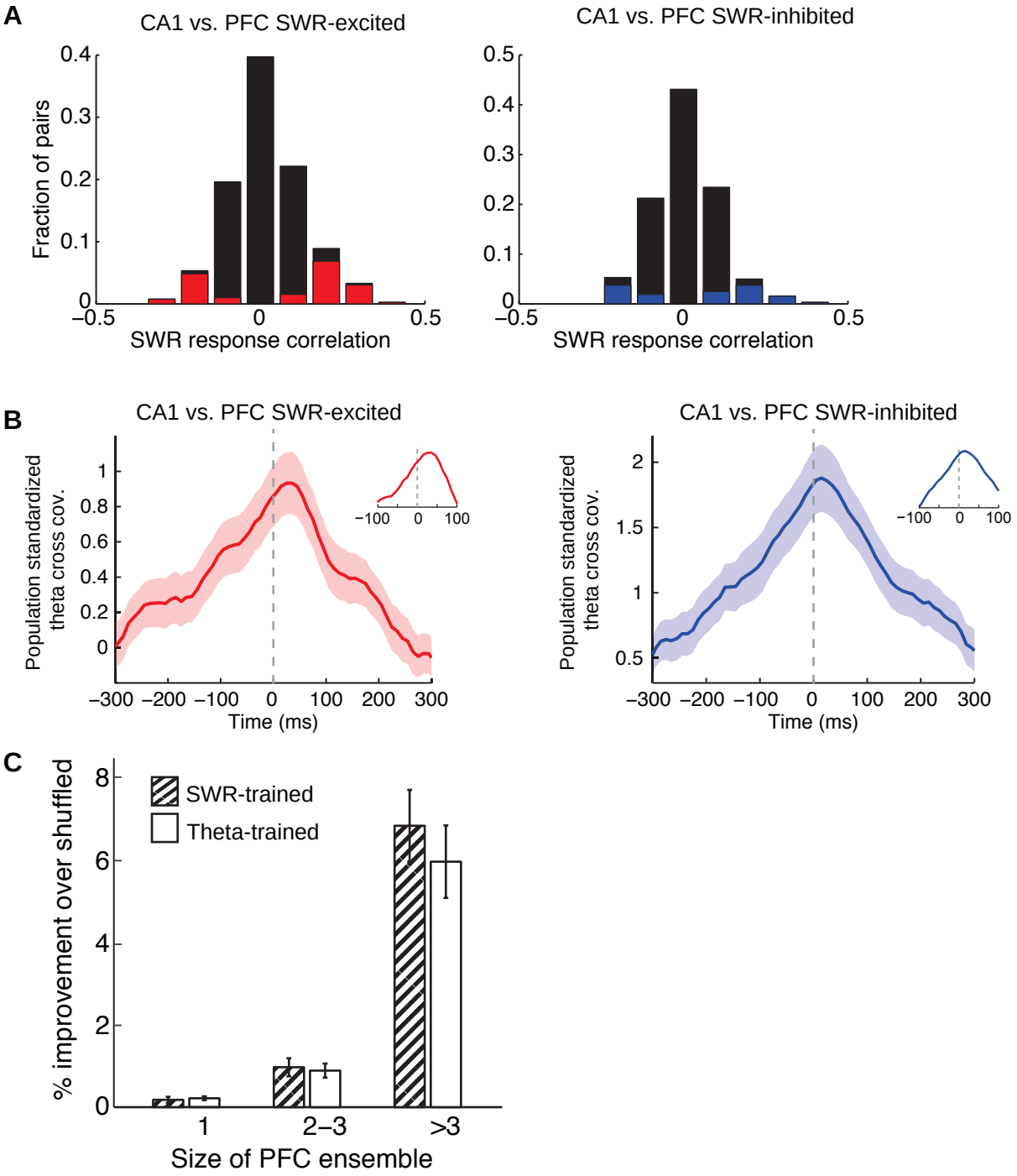
A
CA1 vs. PFC SWR-excited
CA1 vs. PFC SWR-inhibited
Fraction of pairs
SWR response correlation
B
CA1 vs. PFC SWR-excited
CA1 vs. PFC SWR-inhibited
Population standardized theta cross cov.
Time (ms)
C
SWR-trained
Theta-trained
% improvement over shuffled
Size of PFC ensemble
1
2–3
>3

Figure S4

Figure S4 (related to Figure 6): CA1-PFC Reactivation during Awake SWRs.

(A) SWR response correlation distributions for CA1 vs PFC pairs. Colored bars indicate significantly correlated pairs. (*Left*) CA1 vs PFC SWR-excited pairs, n = 393 total pairs, 72 signficant pairs. (*Right)* CA1 vs PFC SWR-inhibited pairs, n = 320 total pairs, 44 significant pairs.

(B) Population standardized cross-covariance during theta periods for CA1-PFC pairs. Only pairs with significant and positive SWR correlations are included. (*Left*) CA1 vs PFC SWR-excited pairs, n = 46 pairs. (*Right*) CA1 vs PFC SWR-inhibited pairs, n = 26 pairs. Insets show area around peaks, illustrating that the peaks after 0 ms for both populations, indicating that CA1 leads PFC on average.

(C) Cross-validated prediction for SWR-associated spiking of CA1 cells using SWR-modulated PFC cells (n = 102 cells total; direction of GLM is reversed as compared to Figure 6E). Prediction was done using PFC ensemble spiking and is plotted as a function of the PFC ensemble size (n = 202, 200 and 80 CA1 cells respectively). SWR-trained (striped bars) prediction performance increased with the size of the PFC ensemble (1-way ANOVA, cell count group: $p< 10^{-10}$). Movement-trained (white bars) prediction performance also increased with the size of the PFC ensemble (1-way ANOVA, cell count group: $p< 10^{-10}$). As expected, predictions using PFC SWR-modulated cells (n = 102) were significantly better than that using PFC SWR-unmodulated (n = 203) cells (SWR-trained model: 2-way ANOVA, p = 0.02, cell count group, $p< 10^{-10}$). As in the CA1-to-PFC model, we found that predictions by PFC SWR-excited and SWR-inhibited cells were similar in the PFC-to-CA1 model (SWR-trained model: 2-way ANOVA, $p > 0.7$, cell count group, $p< 10^{-10}$).

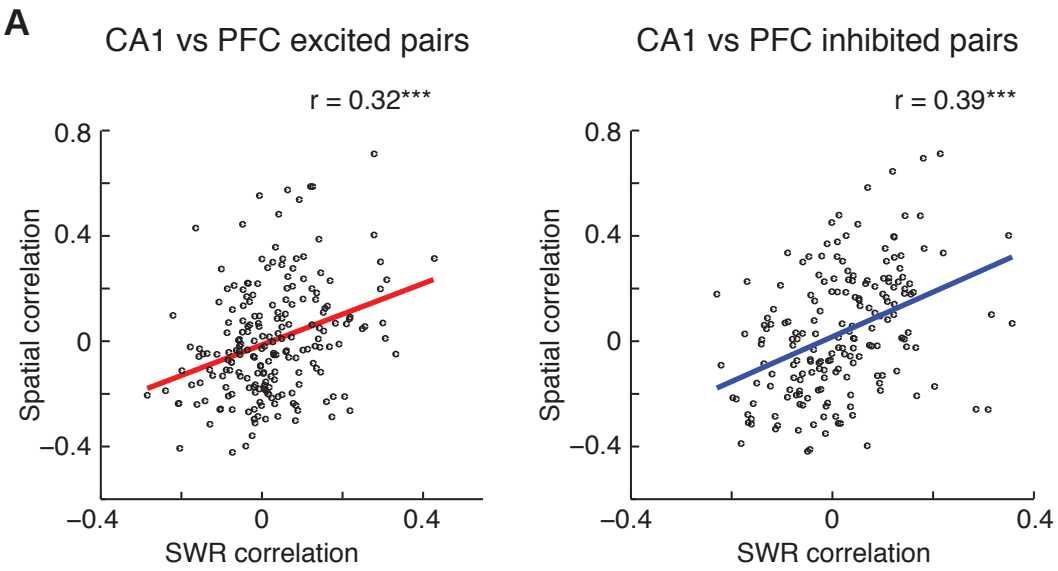

Figure S5

Figure S5 (related to Figure 7): CA1-PFC Spatial Correlations

(A) In order to account for the difference in spatial specificity of SWR-excited and SWR-inhibited neurons, the distribution of spatial specificity of PFC neurons was matched for the two cases using sub-sampling. We only included PFC neurons in pairs for the two cases whose spatial coverages were within the inter-quartile ranges of the values for SWR-inhibited PFC neurons. The spatial correlation of the resulting CA1-PFC pairs in both sub-sets was then compared to their SWR correlation. Both CA1-PFC excited pairs ($n = 203$, $r = 0.32$, $p < 10^{-4}$) and CA1-PFC inhibited pairs ($n = 203$, $r = 0.39$, $p < 10^{-4}$) showed significant correlations. The sub-sampled SWR-excited and SWR-inhibited populations showed similar degree of correlations (shuffle test, $n = 1000$, $p > 0.18$).

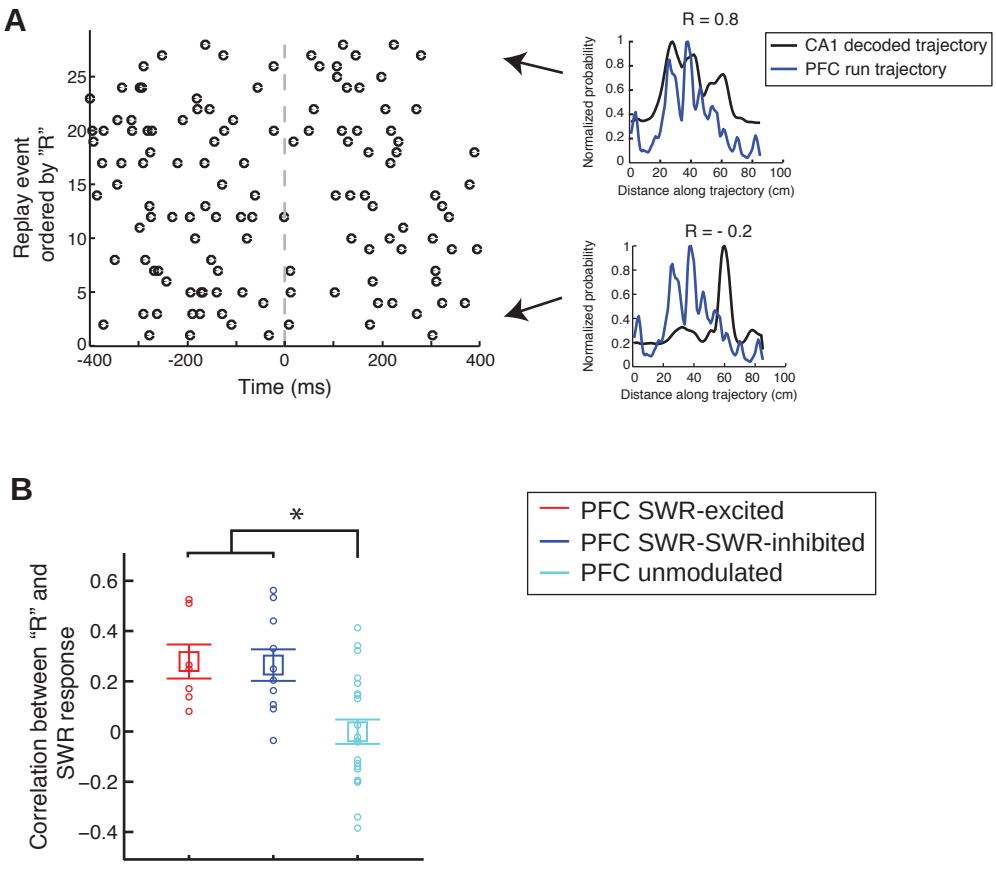

Figure S6

Figure S6 (related to Figure 7): Modulation of PFC Spiking Related to the Content of Hippocampal Replay Events.

(A) We used CA1 ensemble firing during SWRs to decode the replayed spatial trajectories as described previously (*Karlsson and Frank, 2009*). We then asked if a given PFC cell fires more spikes in SWRs during which CA1 replays a set of locations that overlaps with the PFC cell's spatial firing profile (see Experimental Procedures).(*Left*) Raster shows SWR-associated spiking raster of a PFC SWR-inhibited neuron, with the raster ordered by degree of overlap between the decoded CA1 trajectory in each SWR and the spatial firing rate of the PFC neuron in the corresponding trajectory. Examples on *Right* show cases with high and low degree of overlaps between the replayed CA1 trajectory (sum of decoded probability during the entire SWR) and the spatial firing profile of the PFC neuron.

(B) Correlation between the SWR-associated spiking of the PFC neuron and the content of the decoded CA1 locations was significantly higher for SWR-modulated neurons (n = 17 SWR-modulated vs. n = 21 SWR-unmodulated neurons, *p< 0.01, rank-sum test). Note that due to the small number of neurons, the correlation quantified separately for SWR-excited and SWR-inhibited neurons is significantly different than SWR-unmodulated neurons only at the $p < 0.05$ level (n = 7 SWR-excited neurons, n = 10 SWR-inhibited, n = 21 SWR-unmodulated, $p < 0.05$, rank-sum test).

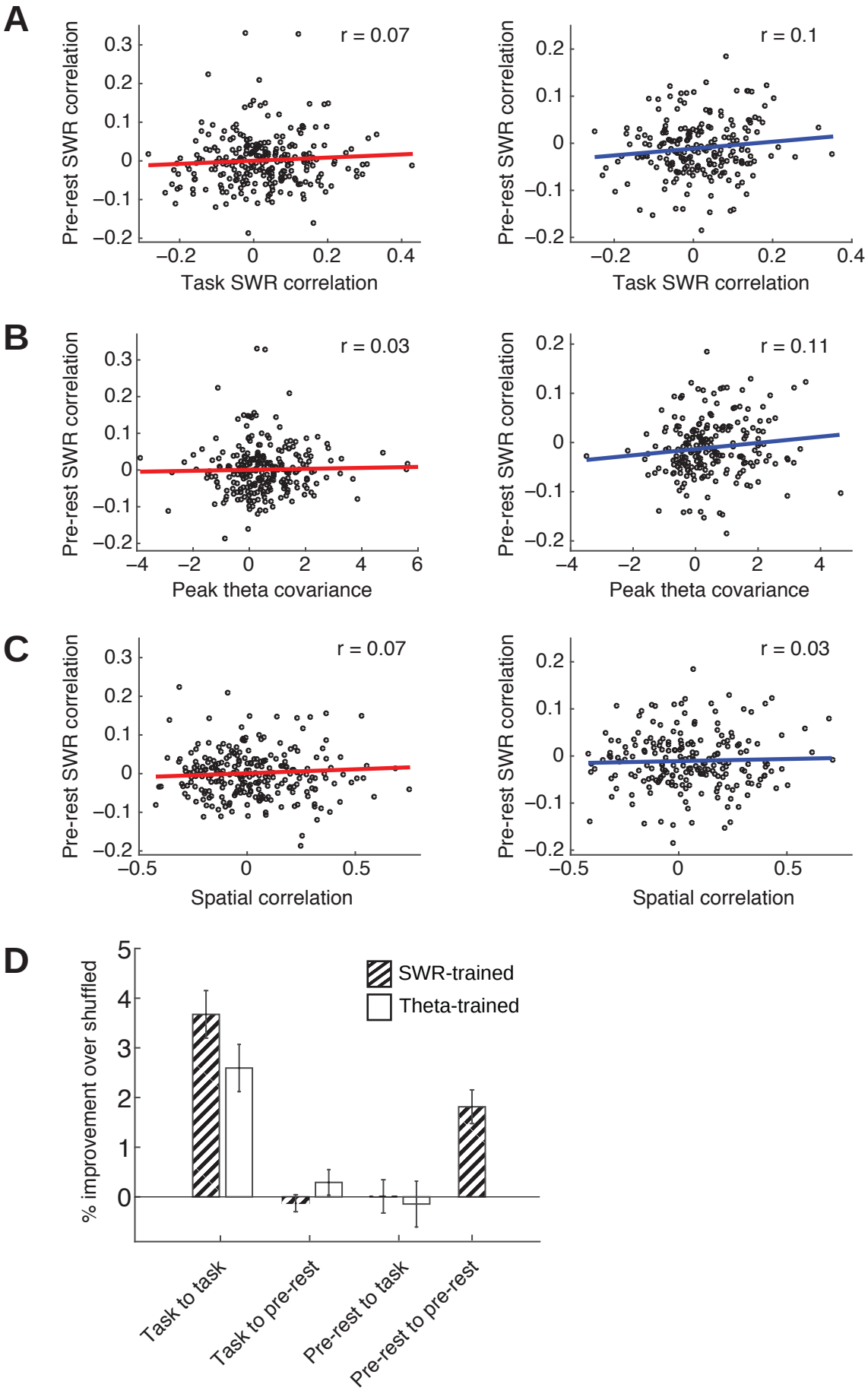
A
r = 0.07
r = 0.1
Pre-rest SWR correlation
Task SWR correlation
B
r = 0.03
r = 0.11
Peak theta covariance
C
r = 0.07
r = 0.03
Spatial correlation
D
SWR-trained
Theta-trained
% improvement over shuffled
Task to task
Task to pre-rest
Pre-rest to task
Pre-rest to pre-rest

Figure S7

Figure S7 (related to Figure 8): Task Related CA1-PFC Correlations are not Present in Preceding Rest Periods for Data Combined for Both Tracks.

(A) SWR response correlation during behavior vs pre-rest periods for CA1-PFC pairs recorded in both epochs. Data is combined for both the W- and the Y- tracks.
(*Left*) CA1-PFC SWR excited pairs (n = 254, r = 0.07, p > 0.2).
(*Right*) CA1-PFC SWR inhibited pairs (n = 211, r = 0.1, p > 0.09).

(B) Peak theta cross-covariance during behavior vs SWR response correlation during pre-rest periods.
((*Left*) CA1-PFC SWR excited pairs (n = 254, r = 0.03, p > 0.6).
(*Right*) CA1-PFC SWR inhibited pairs (n = 211, r = 0.11, p > 0.08).

(C) Spatial correlation during behavior vs SWR response correlation during pre-rest periods.
((*Left*) CA1-PFC SWR excited pairs (n = 254, r = 0.07, p > 0.2).
(*Right*) CA1-PFC SWR inhibited pairs (n = 211, r = 0.03, p > 0.6).

(D) Comparison of cross-validated GLM models for prediction of SWR-associated spiking of PFC cells using CA1 cell activity. Models trained on SWR-activity are represented by striped bars, and those trained on movement activity are represented by white bars, as in Fig. 6E and 8D. The performance of the GLM model is quantified similarly, in terms of the fraction improvement of prediction of real data as compared to shuffled data, only for models that converge (see Supplemental Experimental Procedures). Only significantly SWR-modulated PFC cells during behavior are shown.

Task to task: Using model trained during behavior to predict activity of SWR-modulated PFC cells (n = 77) during behavior. This data corresponds to that shown in Fig. 6E, and is combined for all sizes of the predicting CA1 ensemble.
Task to pre-rest: Using model trained during behavior to predict SWR-associated spiking during pre-rest periods (n = 39 cells). Only PFC cells recorded both in rest and behavior sessions are used. Prediction is only performed if all the CA1 cells used in the model are present in both epochs. Prediction performance was not significantly different from chance (shuffle test, p > 0.5), and was significantly lower than the run-to-run performance (SWR-trained: ranksum test, n = 77 vs. n = 39 cells, $p < 10^{-8}$; Theta-trained: ranksum test, $p < 10^{-6}$).
Pre-rest to task: Using model trained during pre-rest to predict SWR-associated spiking during run periods (n = 42 cells). Prediction performance was not significantly different from chance (shuffle test, p > 0.5), and was significantly lower than the run-to-run performance (SWR-trained: ranksum test, n = 77 vs. n = 42 cells, $p < 10^{-4}$; Theta-trained: ranksum test, $p < 10^{-4}$).
Pre-rest to pre-rest: Using model trained during pre-rest to predict activity during pre-rest (n = 73 cells). Only SWR-trained data is available during pre-rest periods. Prediction performance was significantly lower than run-to-run performance (SWR-trained: ranksum test, n = 77 vs. n = 73 cells, p < 0.01), but significantly higher than either of the two cross-epoch predictions (SWR-trained: ranksum test, n = 73 vs. n = 39 cells, $p < 10^{-4}$; SWR-trained: ranksum test, n = 73 vs. n = 42 cells, $p < 10^{-3}$).

.

Animal	Total excitatory cells		
	CA1 cells	iCA1 subset	PFC cells
W-track			
HPa (1)	195	54	40
HPb (2)	165	15	80
HPc (3)	86	-	51
Sub-total	446	69	172
Y-track			
Ndl (4)	48	-	76
Rtl (5)	113	-	47
Brg (6)	1	-	49
Sub-total	163		171
Total	608	69	343
Cells with < criterion spikes	-72		-31
Total	536		312

Table S1 (related to Figure 1): Cell Distribution Across Animals.

Total number of CA1 and PFC excitatory cells recorded in each animal in the W track task and Y track task. Animal numbers correspond to recording locations shown in **Figure S1**.

Animal	PFC SWR modulation analysis			
	Total PFC cells	PFC excited	PFC inhibited	PFC unmodulated
W-track				
HPa (1)	38	12	11	15
HPb (2)	76	13	9	54
HPc (3)	51	5	6	40
Sub-total	165	30	26	109
		Fraction: 18%	Fraction: 16%	
Y-track				
Ndl (4)	67	18	17	32
Rtl (5)	37	3	8	26
Brg (6)	43	6	1	36
Sub-total	147	27	26	94
		Fraction: 18%	Fraction: 18%	
Total	312	57	52	203
		Fraction: 18%	Fraction: 17%	

Table S2 (related to Figure 3): Distribution of Neurons in PFC SWR Modulation Analysis.

Distribution of PFC cells in the different populations: SWR-excited, SWR-inhibited and SWR-unmodulated categories.

	PFC SWR excited	PFC SWR inhibited	PFC SWR unmodulated	Total
All Cells	57	52	203	312
Theta-modulated	44 (77%)	37 (71%)	108 (53%)	189 (60%)
Theta-unmodulated	13	15	95	123

Table S3 (related to Figure 4): PFC Theta Modulation.

Number of theta modulated PFC cells in the SWR-excited, SWR-inhibited and SWR-unmodulated categories.

SUPPLEMENTAL EXPERIMENTAL PROCEDURES

Animals and Experimental Overview

Six male Long Evans rats weighing 450-550 grams were used in this study. All procedures were approved by the Institutional Animal Care and Use Committee at the University of California, San Francisco and conformed to National Institutes of Health guidelines. Animals were housed singly under a regular 12-hour light/dark cycle. All behavioral experiments were carried out in the light cycle. As previously described (Jadhav et al., 2012), animals were first habituated to daily handling over several weeks. After habituation, animals were food deprived to 85-90% of their baseline weight and pre-trained to run on a raised track for liquid food rewards (evaporated milk), which were automatically dispensed into food wells when the animals interrupted an IR beam above the food well at the ends of the track. Following recovery from surgery and electrode placements, animals were food-deprived and retrained on the pre-training track with the recording cables attached for at least two days before the recording sessions started. During recording sessions, animals either learned to perform a W-track spatial alternation task (Jadhav et al., 2012) (n = 3), or an auditory cue-guided spatial task (n = 3). Following the conclusion of the experiments, we made micro-lesions through each electrode tip to mark recording locations (30 μA for 3 sec). After receiving an overdose of Euthasol, animals were perfused intracardially with isotonic sucrose and 4% PFA. The brains were stored in PFA, frozen, and cut coronally at 50 μm sections, and stained with cresyl violet.

Behavioral Tasks

Animals were trained for 8-12 days, in 2-4 20-minute run sessions per day with interleaving 20-30 minute rest sessions. Data were pooled across all sessions within a day. The tracks were novel on the first day and were made of 7 cm wide metal sections.

Evaporated milk rewards were automatically delivered in food wells triggered by crossing of an IR beam by the rat's nose. The W-track had dimensions of ~80 x 80 cm, with reward food wells at the end of all three arms. Rewards were delivered according to an alternation rule, where the animal had to return to the center well after visits to either side well, and starting from the center well, had to choose the opposite side well from its previous side trajectory. Animals performed 2 sessions on the W-track every day for a total of 8 days. For the auditory-cue guided spatial task, a Y-track was used (84 cm center arm, 64 cm side arms), where following a reward in the home well, in ~75% of trials the rat had to go to the well at the end of the "silent arm" for the next reward. In a pseudo-random ~25% of trials, 5 seconds after poking in the home well, a specific sound was emitted from a speaker, indicating the rat had to go to the well at the end of the "sound arm" for the next reward. The speaker was placed at the end of the sound arm in the first days of training and moved to the center junction after rats displayed consistent correct choices in more than ~70% of trials. Animals typically performed 4 run sessions per day, and auditory protocols were presented in separate rest sessions in the beginning and end of each day.

Surgical Implantation and Electrophysiology

Surgical implantation procedures were as previously described (Jadhav et al., 2012). Animals were implanted with a microdrive array with 21 independently moveable tetrodes (groups of four twisted 12.5 μm nichrome wires) assembled in a bundle. In animals performing the W-track task, the bundles targeted right dorsal hippocampal region CA1 (-3.6 mm AP and 2.2 mm ML), right PFC (+3.0 mm AP and 0.7 mm ML, 5 degree angle in one animal), and intermediate CA1 (-6.3 mm AP and 5.5 mm ML, in two animals). In the animals performing the auditory-cue guided Y-track spatial task, the bundles targeted left dorsal CA1 (-3.6 mm AP and -2.2 mm ML) and left PFC (+3.0 mm

AP and -1 mm ML). Recordings were also carried out in primary auditory cortex (-4.8mm AP and -5.5 mm ML, 25 degrees lateral from midline). In one animal on the Y-track, we were able to record only 1 CA1 cell along-with 49 PFC cells, although LFP recordings were obtained from dorsal CA1. **Figure S1** shows the recording location for all electrodes in all animals, and distribution of cells across animals is shown in **Table S1**. The majority of neurons were recorded in dorsal CA1 (n = 538), and a small minority in intermediate CA1 (n = 70). Only data from hippocampal and prefrontal recordings are reported here, and we pooled together data from all the animals.

On the days following surgery, hippocampal tetrodes were advanced to the cell layers until characteristic EEG patterns (sharp wave polarity, theta modulation) and neural firing patterns indicated that the target regions had been reached. PFC tetrodes were advanced gradually to the desired depth (~3 mm from bregma), and were adjusted after daily recording sessions if necessary. For hippocampal tetrodes, spiking activity was recorded relative to a reference tetrode located in the corpus callosum, and for PFC tetrodes, spiking activity was recorded either relative to the corpus callosum reference tetrode, or a reference tetrode in overlying cortical regions.

Data were collected using the NSpike data acquisition system (Jadhav et al., 2012; Karlsson and Frank, 2009) (L.M.F. and J. MacArthur, Harvard Instrumentation Design Laboratory). We recorded continuous local field potentials (LFP, filtered 0.5-400 Hz and sampled at 1500 Hz) from all tetrodes (one channel was chosen from each tetrode for LFP recording). Spike data were sampled at 30 kHz, digitally filtered between 300 or 600 Hz and 6 kHz (2 pole Bessel for high and low pass) and threshold crossing events were saved to disk (40 samples at 30 kHz). An infrared light emitting diode array with a large and a small cluster of diodes was attached to the preamps during recording.

Behavior sessions were recorded with an overhead monochrome CCD camera (30 fps) and the animal's position and speed were detected online using the infrared diodes.

Data Analysis

Data analysis was performed using custom routines in Matlab (MathWorks, Natick, MA). We used non-parametric tests for statistical comparisons throughout the manuscript unless otherwise noted. All values reported are mean ± sem unless otherwise noted. For tests with multiple comparisons between SWR-excited, SWR-inhibited and SWR-unmodulated PFC neurons, we set the threshold p-value at 0.01 (*p< 0.01, **p< 0.001).

SWR Detection

All analyses were performed using custom code written in Matlab (MathWorks, Inc.). SWRs were detected using LFPs filtered in the 150-250 Hz range on multiple CA1 tetrodes as previously described (Karlsson and Frank, 2009). Increases in power in the ripple band were detected using a 3 s.d. criterion. A speed criterion of < 4 cm/sec was also applied to avoid any spurious detection of high frequency fast gamma episodes which occur during running (Kemere et al., 2013). Further, we discarded all SWRs that occurred within 1 sec of a previously detected SWR, ensuring unambiguous assignment of PFC spikes with respect to SWR onset time. A total of 19,888 SWRs were recorded over 53 days (mean ± sem = 381 ± 18 per day). The average duration of SWRs was 96.7 ± 1.2 ms (n = 19,888 SWRs), and the average SWR rate was 0.12 ± 0.01 Hz (n = 53 days of recording).

SWR Modulation

We limited our analysis to putative PFC excitatory neurons with a criterion of at least 50 spikes occurring in SWR-aligned rasters (aligned to SWR onset) during the recording

session on each day. Fast-spiking (FS) putative inhibitory interneurons (n = 10) were detected by a consistent spike width and firing rate criterion across the two tasks (spike-width < 0.3 ms and firing rate > 17 Hz) and excluded from further analysis. A further 31 cells were excluded as they did not have sufficient number of spikes (< 50) for quantification of SWR modulation. This analysis therefore included a total of 312 PFC neurons. Similarly for CA1 neurons, FS neurons (n = 22, spike-width < 0.3 ms and firing rate > 7 Hz), and cells with less than 50 spikes in SWR-aligned rasters (n = 72) were excluded, and a total of 536 CA1 cells were used in the analysis. All our results were similar with exclusion of intermediate CA1 cells (n = 70), or for analyses limited to the W-track (data not shown).

SWR-modulation metric: for each PFC neuron we first averaged its SWR-triggered raster to yield a peri-SWR time histogram (SWR-PSTH). We then created 5000 shuffled SWR-PSTHs, each one constructed by circularly jittering the spikes around each SWR by a random amount (all spikes around the same SWR were shifted by the same fixed time). We calculated the squared difference between the real SWR-PSTH and the mean of the shuffled SWR-PSTHs in the 0-200 ms window after SWR onset, to obtain a SWR-modulation measure. To determine SWR-modulation significance, we calculated SWR-modulation measures in the same way for the 5000 shuffled SWR-PSTHs. If the SWR modulation measure of the real SWR-PSTH was greater than 95% of the shuffled PSTHs, the PFC neuron was determined to be SWR-modulated. Using this criterion, we found 57/312 SWR-excited PFC neurons, 52/312 SWR-inhibited neurons, and 203/312 SWR-unmodulated PFC neurons (neurons which did not satisfy this modulation criterion). Using a similar criterion for CA1 cells, we found 429/ 536 cells to be SWR-modulated. PFC SWR-modulated neurons were categorized as SWR-excited or SWR-inhibited by comparing the rate in the 0-200 ms window after SWR onset with the rate in a pre-SWR background window -500 to -100 ms window before SWR onset.

Timing of SWR-response: Peak or trough time for each cell was based on the average SWR-PSTH. The distribution of peak times across neuron categories was compared using a ranksum test. The rise or fall time was defined as the time when the SWR-PSTH first increased or decreased 1 standard deviation away from the mean. The cross-covariance for CA1 vs. PFC SWR-excited cells and CA1 vs. PFC SWR-inhibited cells were generated from the SWR-aligned rasters, and adjusted for mean firing rates of the neurons.

Theta Phase Locking

Theta phase-locking was calculated using the methods developed in previous reports (Siapas et al., 2005). Theta oscillations were filtered in the 6-12 Hz range in the LFP down-sampled to 150 Hz. We used a CA1 tetrode located in corpus callosum as reference theta phase, since theta phase has been reported to be constant in depth above the CA1 cell layer (Lubenov and Siapas, 2009). Theta periods were assigned based on a speed criterion of >5 cm/sec and no SWRs detected on any of the CA1 tetrodes with a 3 s.d. criterion. Phase-aligned histograms were generated by aligning spikes from individual neurons to reference theta phase, and spikes were assigned a phase between 0-360° using these histograms. Only neurons with at-least 50 spikes in the theta-aligned histograms were included in the analysis. Deviations from the circular uniform distribution were detected in the individual neuron phase distributions using the Rayleigh test of uniformity ($p < 0.05$ criterion). A circular concentration parameter (κ), which quantifies the strength of the phase locking, was estimated by fitting these phase distributions to a von Mises distribution. SWR modulation and theta phase locking was compared for neurons with both measures defined in different categories (PFC SWR-excited, PFC SWR-inhibited, PFC SWR-unmodulated).

Spatial and Behavioral Coding Properties

Spatial firing properties of neurons were computed using occupancy-normalized linearized firing rates of neurons (**Figure 5, S3, 7**). We constructed occupancy normalized linear firing rate maps for each neuron from spike times and the two-dimensional animal position, projected onto the 4 linear trajectories on the track. Spatial coverage of neurons was defined as the fraction of area above 25% of the peak firing rate of the neuron defined across all 4 trajectories (neurons with a threshold peak firing rate > 3 Hz). Arm Index was defined as the absolute difference between left and right arm firing rates, normalized by the sum of the firing rates (range between 0-1). Similarly, direction index was defined as the absolute difference between outward and inward arm firing rates, normalized by the sum of the firing rates. Spatial correlations between neurons (**Figure 7**) were also calculated using the linearized firing rates. To calculate firing rate modulation between SWR as compared to high speed periods (**Figure 5F**), we calculated a pre-SWR firing rate in a -500 to -100ms time window before SWR onset, and a high-speed firing rate for speeds > 10 cm/sec. The firing rate modulation was then defined as (pre-SWR rate – high speed rate)/ (pre-SWR rate + high speed rate), yielding a normalized index that varies between -1 to +1:. Firing rate modulation by reward (**Figure S3**) was calculated similarly. Spiking of PFC neurons was aligned to time of reward (extracted for each trajectory from the position and speed data) to generate reward-aligned rasters and PSTHs. Firing rate modulation was calculated using a post-reward firing rate in a 0 to 2 second time window after reward, and a pre-reward firing rate in a -3 to -1 second window prior to reward. The reward modulation index was then calculated as a (post-reward rate – pre-reward rate)/ (post-reward rate + pre-reward rate).

SWR Correlations and Theta Cross-covariance

SWR correlations between pairs of CA1-PFC neurons were measured as the correlation coefficient between the magnitudes of the spiking responses of the two neurons in the 0-200 ms aligned to SWR onset. Only pairs (n = 713) with at-least 5 simultaneous events (at-least 1 spike from each cell in the pair in SWR response window, 0-200 ms) were included in the analysis. The significance of the fraction of pairs with significant SWR correlations (~16%, n = 116/ 713) was determined using a Z-test for proportions. Compared to shuffled data (~5% pairs significant after shuffling rates across SWRs), z = 6.5, and $p < 10^{-8}$. Proportions were also calculated separately for pairs with PFC SWR-excited cells (n = 393), and pairs with SWR-inhibited cells (n = 320), and are reported in the text and figures.

Standardized cross-covariance during theta (**Figure 5** and **6**) was calculated similar to previous reports (Siapas et al., 2005). Only theta periods that were at-least 1 second long were included in the analysis. Theta periods were assigned as above based on a speed criterion of >5 cm/sec and no SWRs detected on any of the CA1 tetrodes with a 3 s.d. criterion. First, the cross-correlation histograms were computed for pairs of neurons using 10 ms bins, and the cross-covariance estimated by subtracting the expected rate of coincidence in each bin based on the mean firing rates. The standardized (or Z-scored) cross-covariance was then calculated by normalizing the cross-correlation by the mean firing rates of the neurons, the bin size, and the total length of the theta period. The peak of the smoothed standardized theta cross-covariance (smoothing using a Gaussian of length 50 ms and a standard deviation of 16.7 ms) was determined in a -200 to +200 ms window around zero lag.

Spatial correlations between neurons (**Figure 7, S5**) were calculated using the linearized firing rates as described above. The relationship between spatial correlation and SWR correlation for PFC SWR-excited and SWR-inhibited neurons was compared using a shuffle test. Each correlation was compared to a mixed distribution with the

same number of cell pairs that was generated randomly from both datasets, and the actual correlation was compared to the correlation of the mixed populations (n = 1000) to generate a p-value.

GLM

For each PFC neuron, we trained a generalized linear model (GLM) with a log link function to predict SWR-related spiking of that PFC neuron from the activity of the simultaneously recorded CA1 ensemble. The summed spiking activity of each neuron in the 0-200 ms window after SWR onset was considered as the SWR-response. PFC neurons and corresponding CA1 ensembles for which the GLM did not converge (largely due to insufficient data) were removed from further analysis. To determine predictive significance, we used a cross-validation approach. A GLM was trained on 90% of the SWR-responses, and the obtained beta coefficients were used to predict the PFC SWR-response from CA1 responses of the remaining 10% of SWRs. The prediction error was estimated as the mean absolute difference in estimated spiking from the actual measured spiking. A “shuffled” prediction error was obtained by shuffling predicted responses across SWRs. This procedure was repeated 5000 times, each time on randomly chosen 90%/10% of the data. For predicting PFC SWR-responses from CA1 SWR-responses using a model trained on behavior data, we binned all the spiking activity during behavior (animal moving faster than 5 cm/ sec, no SWRs) into 200 ms bins. This data was similarly used to train GLM models, and the obtained beta coefficients were used to predict PFC SWR-response from the CA1 SWR-responses. Similarly, SWR-trained models were used to predict PFC behavioral data from the CA1 behavioral data. In the reverse analysis (**Figure S4**), we used a GLM model to predict spiking of a CA1 neuron from the activity of the simultaneously recorded PFC ensembles

in each category (SWR-modulated, SWR-excited, SWR-inhibited and SWR-unmodulated PFC cells).

Replay analysis

We used CA1 ensemble firing during SWRs to decode the replayed spatial trajectories as described previously (Karlsson and Frank, 2009). Briefly, only SWRs with at-least 4 CA1 cells spiking during SWRs were considered candidate events. The spatial probability in each 15 ms bin during the SWR was decoded from the corresponding CA1 spikes in that bin using Bayesian methods and assuming a Poisson distribution for spiking. The significance of the decoded replay event was then assessed by asking if the decoded event represented a series of spatial locations on a trajectory as compared to shuffled data (shuffling procedure for the time bins with n = 500 total shuffles). Only events with $p < 0.05$ criterion were considered as significant events and used for further analysis. We then compared the decoded spatial probability based on CA1 replay to the firing profile of a PFC neuron in the corresponding trajectory. Only PFC neurons with at-least 10 corresponding significant replay events were included in this analysis. The correlation between these spatial probabilities (decoded CA1 event vs. firing profile of PFC neuron on corresponding trajectory) was compared to generate an "R" value for each neuron. The "R" value quantifies the degree to which the SWR-associated spiking of a PFC neuron is modulated by the content of the replay event.

Task and rest period comparisons

To compare CA1-PFC relationships seen during behavior to those in pre-task periods, we only used cells that were recorded in both pre-task (also termed *pre-rest*) and behavioral epochs. Animals were placed in a rest box during these pre-task sessions as described above. Analysis was performed separately for the W-track behavior (**Figure**

8), and with data combined from both W-track and Y-track behavioral tasks (**Figure S7**). PFC cells were categorized similarly to other analyses as SWR-modulated or unmodulated based on their responses during behavior. SWRs were detected in pre-task epochs similarly to behavioral epochs. SWR response correlations in CA1-PFC pairs during pre-task periods were compared to SWR correlations during behavior, as well as theta covariances and spatial correlations during behavior. For GLM model comparisons, models were trained using behavioral data to predict PFC SWR spiking using CA1 ensemble spiking. These same models were then used to predict pre-task SWR data. The reverse analysis used models trained on pre-task data to predict behavioral data. The prediction performances of these cross-epoch GLMs were compared to cross-validated models (as described above) that used data within the same epoch for training and validation.

Supplemental References

Jadhav, S.P., Kemere, C., German, P.W., and Frank, L.M. (2012). Awake hippocampal sharp-wave ripples support spatial memory. Science *336*, 1454-1458.

Karlsson, M.P., and Frank, L.M. (2009). Awake replay of remote experiences in the hippocampus. NatNeurosci *12*, 913-918.

Kemere, C., Carr, M.F., Karlsson, M.P., and Frank, L.M. (2013). Rapid and continuous modulation of hippocampal network state during exploration of new places. PLoS One *8*, e73114.

Lubenov, E.V., and Siapas, A.G. (2009). Hippocampal theta oscillations are travelling waves. Nature *459*, 534-539.

Siapas, A.G., Lubenov, E.V., and Wilson, M.A. (2005). Prefrontal phase locking to hippocampal theta oscillations. Neuron *46*, 141-151.